UC Berkeley
UC Berkeley Previously Published Works

Title

Tired and misconnected: A breakdown of brain modularity following sleep deprivation

Permalink

https://escholarship.org/uc/item/4z99652n

Journal

Human Brain Mapping, 38(6)

ISSN

1065-9471

Authors

Simon, Eti Ben

Maron-Katz, Adi

Lahav, Nir

et al.

Publication Date

2017-06-01

DOI

10.1002/hbm.23596

Copyright Information

Peer reviewed

Tired and Misconnected: A Breakdown of Brain Modularity Following Sleep Deprivation

Eti Ben Simon [iD],[1,2]* **Adi Maron-Katz,**[1,2] **Nir Lahav,**[3] **Ron Shamir,**[4] **and Talma Hendler**[1,2,5,6]

[1]*Functional Brain Center, Wohl Institute for Advanced Imaging Tel-Aviv Sourasky Medical Center, Tel Aviv, Israel*
[2]*Sackler Faculty of Medicine, Tel Aviv University, Tel Aviv, Israel*
[3]*Department of Physics, Bar-Ilan University, Ramat Gan, Israel*
[4]*Blavatnik School of Computer Science, Tel-Aviv University, Tel-Aviv, Israel*
[5]*School of Psychological Sciences, Tel Aviv University, Tel-Aviv, Israel*
[6]*Sagol school of Neuroscience, Tel Aviv University, Tel Aviv, Israel*

Abstract: Sleep deprivation (SD) critically affects a range of cognitive and affective functions, typically assessed during task performance. Whether such impairments stem from changes to the brain's intrinsic functional connectivity remain largely unknown. To examine this hypothesis, we applied graph theoretical analysis on resting-state fMRI data derived from 18 healthy participants, acquired during both sleep-rested and sleep-deprived states. We hypothesized that parameters indicative of graph connectivity, such as modularity, will be impaired by sleep deprivation and that these changes will correlate with behavioral outcomes elicited by sleep loss. As expected, our findings point to a profound reduction in network modularity without sleep, evident in the limbic, default-mode, salience and executive modules. These changes were further associated with behavioral impairments elicited by SD: a decrease in salience module density was associated with worse task performance, an increase in limbic module density was predictive of stronger amygdala activation in a subsequent emotional-distraction task and a shift in frontal hub lateralization (from left to right) was associated with increased negative mood. Altogether, these results portray a loss of functional segregation within the brain and a shift towards a more random-like network without sleep, already detected in the spontaneous activity of the sleep-deprived brain. *Hum Brain Mapp 38:3300–3314, 2017.*   © 2017 Wiley Periodicals, Inc.

Key words: sleep deprivation; fMRI; modularity; amygdala; mood; functional connectivity; graph theory

---

INTRODUCTION

Sleep deprivation (SD) has been associated with various cognitive and affective impairments ranging from decreased executive attention [Dinges et al., 1997] to increased emotional reactivity [Zohar et al., 2005] and worse mood [Pilcher and Huffcutt, 1996]. These changes were later associated with altered activity patterns in executive prefrontal regions [Drummond et al., 2005] as well as in core regions of the limbic system, such as the amygdala [Simon et al., 2015; Yoo et al., 2007]. For instance, several neuroimaging studies have now shown that SD results in hyper activation

of the amygdala typically coupled with reduced amygdala-prefrontal connectivity (see review by Goldstein and Walker [2014]). Interestingly, resting-state studies have also revealed significant alterations in the connectivity profile of the amygdala following 36 h of SD, reflecting preexisting changes in limbic network connectivity, prior to any task performance [Lei et al., 2015; Shao et al., 2014]. Changes in resting thalamic connectivity were also detected following SD, demonstrating a reduction in thalamic connectivity with multiple temporal and prefrontal regions [Shao et al., 2013], thought to reflect substantial changes in vigilance without sleep.

Beyond region specific connectivity, sleep deprivation has also been associated with reduced connectivity within the default mode, dorsal attention, auditory, visual and motor networks [Gao et al., 2015; Kaufmann et al., 2016; Yeo et al., 2015]. In fact, changes to resting whole-brain connectivity patterns following one night of sleep loss are so robust, they allow for the successful classification of sleep state (deprived vs. rested), with over 60% accuracy [Kaufmann et al., 2016].

Beyond this accumulating evidence on the network-level effects of sleep deprivation, it still remains unclear how such changes ultimately shape the brain's global functional organization when deprived of sleep. Graph theory studies have shown that the brain is functionally organized into distinct modules [Bullmore and Sporns, 2009], which are further maintained across sleep stages [Tagliazucchi et al., 2013]. Functional modules are identified by grouping regions in a way that maximizes the number of within-group links while minimizing the number of between-group links, reflecting the network's ability to maintain functional segregation [Bullmore and Sporns, 2009]. Graph theory tools can therefore offer, for the first time, a global insight into the brain's intrinsic functional organization without sleep. Examined from this perspective one can portray the global functional "trends" inflicted upon the network without sleep and their association with behavior.

To this end, we constructed functional graphs from resting fMRI data of 18 healthy participants acquired both under sleep rested (SR) and sleep deprived (SD) states. Graphs were formed using a predefined functional parcellation [Craddock et al., 2012], with each of the 200 regions of interest (ROIs) defined as nodes, while edges were set by thresholding functional connectivity levels between node pairs. To examine key changes in functional segregation without sleep these graphs were further subdivided into stable functional modules in a data driven manner [Maron-Katz et al., 2016a], allowing for an effective examination of network modularity.

Given earlier reports of reduced functional connectivity across several networks following sleep loss, we hypothesized that SD would induce a significant change in the brain's modularity structure, leading to a loss of functional segregation and a reduction in network modularity. These changes were further hypothesized to mirror cognitive and emotional impairments known to occur without sleep.

To look into affective changes, we examined behavioral indices of emotional state (mood questionnaires) and their association with graph measures of affective networks. Cognitive impairments were assessed using the psychomotor vigilance task (PVT, [Chee et al., 2008]), known to be impaired by low vigilance and sleepiness, and their association with graph measures of attentional networks.

MATERIALS AND METHODS

Participants and Study Design

Eighteen adults (age range: 23–33 years, mean 26.9 ± 3 years; 10 females) completed a within subject paired design across SD and SR sessions. Participants were healthy with no prior history of sleep, neurologic or psychiatric disorders. Recent use of psycho-stimulants (e.g. Ritalin), psychiatric or hypnotic drugs or high caffeine consumption (>3 cups a day) also excluded subjects from participation in the study. Normal sleep-wake patterns were further validated using actigraphy as well as subjective sleep logs. The study was approved by the Tel-Aviv Sourasky Medical Center's ethical review board and all participants provided written informed consent.

Study design was the same as described in our previous work [Simon et al., 2015]. Briefly, participants took part in two experimental sessions: once after a night of normal sleep (i.e. the sleep-rested condition) and again following 24 h of supervised SD. Participants had to abstain from alcohol and caffeine 2 days prior to each session as well as throughout the SD night. For the SD session, participants reported to the lab at 22:30 p.m., typically at the end of a working day, and were continuously monitored by the research staff. Starting from 23:00, and every 2 h, participants performed a battery of questionnaires assessing sleepiness and mood (detailed below). The SD session typically included two subjects in the same night and activity protocol was kept in accordance with our previous work [Simon et al., 2015]. At approximately ∼08:30 a.m. (±90 min) in the following morning of each session participants entered the MRI scanner. Test sessions were separated by a mean of 13.8 days with the order of the SR-SD sessions counterbalanced across participants.

Scanning Session and Behavioral Measurements

In each experimental session, we acquired an fMRI resting-state scan in which subjects were instructed to stay awake and keep their eyes open on a fixation cross. Subjects' eyes were continuously monitored using a dedicated camera to ensure compliance to these instructions. The rest scan lasted for 6:50 min and was performed at the same time of the day in both sessions (∼8:30 a.m.), to avoid circadian effects. Furthermore, the rest scan was performed before any subsequent task performance to minimize possible impact of prior task performance on the resting-state

data [Barnes et al., 2009; Liang et al., 2013]. Following the rest scan, subjects performed an emotional distraction task, the results of which have been published elsewhere [Simon et al., 2015]. Since this task revealed amygdala hyper activation following SD, its results were further used in our post hoc analysis to examine the link between rest and task evoked changes in affective networks without sleep (see details below and in the Supporting Information).

Cognitive and behavioral changes as a function of sleep were further monitored across both experimental sessions. To assess changes in cognitive performance participants completed a 10-min version of the known Psychomotor Vigilance Task [Drummond et al., 2005] (PVT) using the PEBL task library [Mueller and Piper, 2014] every 2 h during the SD night (from 23:00 until 7:00 a.m.) as well as upon arrival at the sleep-rested session. To track mood changes, the Positive and Negative Affective Scale (PANAS [Watson et al., 1988]) was administered every 4 h across the SD night as well as upon arrival at the sleep-rested session. The PANAS consists of two 10-item questionnaires assessing either positive or negative affect, that are rated on a scale ranging from 1 to 5.

fMRI Preprocessing and Parcellation

Imaging was performed on a 3T General Electric (GE) Horizon echo speed scanner with a resonant gradient echo planar imaging system (GE, Milwaukee, WI). All images were acquired using a standard head coil. The scanning session included functional T2*-weighted images (FOV = 220 mm, matrix size = 96 × 96, voxel size: 3 × 3 × 4, TR/TE = 2,500/35, slice thickness = 4 mm, 32 slices without gap, oriented according to the fourth ventricle, flip angle 90°) and a three-dimensional (3D) anatomical scan using T1 SPGR sequence (1 × 1 × 1 mm). SPM8 software (http://www.fil.ion.ucl.ac.uk/spm) was used for image preprocessing as well as voxel-based statistical analysis. The first 18 s of the functional data were discarded to allow steady-state magnetization. Functional images were motion corrected and slice time corrected, realigned to the first scan and normalized according to standard MNI space. Due to excessive head movements in both scans (>2 mm) one subject had to be excluded from further analysis and thus the fMRI analysis includes 17 subjects. Spatial smoothing was performed utilizing a Gaussian kernel (FWHM = 6 mm).

Before further analysis, images were corrected for physiological noise by band-pass filtering to eliminate signals outside the range of 0.01 to 0.08 Hz [Joyce et al., 2013; van den Heuvel et al., 2008] using the REST toolbox [Song et al., 2011]. To parcel the brain into multiple regions of interest (ROIs) we used a whole brain functional parcellation reported in [Craddock et al., 2012], which partitions the brain volume into 200 parcels or ROIs. This parcellation was originally generated by applying a correlation-based clustering procedure on resting state fMRI data recorded from 41 healthy subjects [Craddock et al., 2012]. Parcels

were further masked to include only gray matter voxels using the WFU Pick Atlas Tool [Maldjian et al., 2003; Stamatakis et al., 2010]. As a result, 18 parcels with less than five voxels in common with the gray matter mask were excluded, leaving a total of 182 ROIs.

For each subject, average BOLD signal across all gray matter voxels was calculated within each parcel at the two rest sessions separately (SR and SD). This time series was used as the parcel's signal. In order to reduce the effects of physiological artifacts and nuisance variables, six motion parameters, cerebrospinal fluid, and white matter signals were regressed out of the parcels' signal. The residuals of these regressions comprised the set of mean time courses used for all downstream analysis. Given the impact of head motion on functional connectivity measures [Power et al., 2012], we further examined whether subjects' movement parameters were different across SD and SR states. For each subject, we calculated the number of relative movements (i.e. from each TR to the next) larger than 1 mm separately for each state. We found no significant differences across sleep states (means ± STD: SR 0.1176 ± 0.3321; SD 0.2941 ± 0.5879; P = 0.5, Wilcoxon-signed rank sum test). We further examined the correlation between mean relative head movement and the difference in modularity scores (ΔQ, both SD-SR), to ensure that movement parameters were not associated with the change in modularity across participants. We found no significant correlation between the difference in relative head movement across states and the change in modularity scores (Spearman correlation coefficient r = 0.21, P > 0.4).

Additionally, in order to ensure that motion related artifacts did not affect our main finding, we repeated the modularity analysis using scrubbed data (scrubbing relative movement > 0.5 mm in accordance with [Power et al., 2014]). We found no difference in modularity scores across scrubbed vs. unscrubbed data in either state (mean (ΔQ): SR = 3.5839e-04, P = 0.5618; SD = 0.004, P = 0.1859; both Wilcoxon-signed rank sum test). Furthermore, a significant difference in modularity across sleep states was still evident following scrubbing (Q, mean (ΔQ) = −0.036, P < 0.01, Wilcoxon-signed rank sum test).

Of note, we did not apply global signal removal, a practice that has been under debate in the last few years due to its propensity to produce artificial deactivations [Murphy et al., 2009], particularly in the white matter and cerebrospinal fluid [Greicius and Menon, 2004]. A full discussion on this topic can be further found in [Laurienti, 2004]. It is important to note that SD states in particular [Yeo et al., 2015] and drowsiness in general [Wong et al., 2013] have been shown to alter global signal modulations and its removal might therefore obscure highly relevant functional changes induced by SD. In accordance, attempting to classify SD-SR states using the LOCCV procedure (see below) resulted in lower classification accuracy after global signal removal (see Supporting Information for further details).

Graph Construction

In order to construct a whole-brain graph the following steps were performed: first, for each subject and state, pairwise functional connectivity (FC) matrices were computed based on the Pearson correlation coefficients [Lee Rodgers and Nicewander, 1988] between the BOLD time-course of each parcel/ROI pair. Hence the ROI-ROI for correlations for all pairs define a symmetric correlation matrix C whose (i, j) element is the correlation between ROIs i and j. These matrices were then used to construct an unweighted, undirected graph G for each subject in each state by applying a threshold Θ on C. The nodes of G are the set of all ROIs, and an edge between nodes i and j exists if $C(i,j) > \Theta$. The correlation threshold Θ was determined using link density d, defined as the fraction of possible edges present in the graph.

The link density d was chosen as to maximize the classification accuracy between SD and SR graphs. We tested each value of d in the range of 0.01 to 0.2 in 0.01 intervals. Sleep state classification was achieved using leave-one-out cross validation (LOOCV) analysis as follows: on each iteration subject s is excluded, and the average graph over the remaining subjects is computed by including only edges that appear in the majority (at least 50%) of the subjects. This is done separately on the SR and SD graphs. Each of the two graphs of subject s is then classified as either SR or SD based on its similarity to the two average group graphs. We used the Jaccard score to measure the similarity between graphs. Given two graphs with the same set of nodes (i.e. parcels) G1(V, E1), G2(V, E2), the Jaccard score between E1 and E2 is defined as follows:

$$\mathrm{jac}(G1, G2) = \frac{|E1 \cap E2|}{|E1 \cup E2|} \quad (1)$$

For each subject s, a success function was defined as described below in equation (2). In this function G_s is the graph for subject s, and G_{-s} is the average graph for the remaining subjects.

Total success level (suc) was defined as:

$$\mathrm{suc} = \sum_{s=1}^{\mathrm{subs}} \mathrm{Success(s)}$$

Its significance was evaluated using the binomial cumulative distribution function, with $P = 0.5$, $n = 2 \times$ subjects:

The binomial cumulative distribution function is as follows:

$$p(\mathrm{suc} \geq k) = \sum_{i=k}^{n} \binom{n}{i} 0.5^n$$

Classification Optimization via Feature Selection

In order to identify ROIs that are most relevant to distinguishing between SD and SR states, we repeated the SD-SR classification using only a subset of the ROIs (i.e. the graph nodes). In a LOOCV procedure, each iteration involved exclusion of one subject s, and ranking of the nodes according to the absolute difference in average group-level values between the two states (with subject s excluded). Each of the left-out graphs was assigned to either SR or SD state to whose k-length average degree vector it was closer. Analysis was performed using k top ranking nodes with $k = 1$ to 182. Accuracy levels were defined as the fraction of correct assignments. Sensitivity was defined as the fraction of correctly assigned SD matrices, while specificity was defined as the fraction of correctly assigned SR matrices.

Examining Changes in Graph Modularity

The Brain Connectivity Toolbox (BCT) [Rubinov and Sporns, 2010] was used to examine changes in network modularity. The modularity of a graph is a measure of functional segregation, and reflects the degree to which a network can be clearly partitioned into delineated subgroups [Newman and Girvan, 2004; Rubinov and Sporns, 2010; Rubinov and Sporns, 2011]. It is measured by using the modularity quality function/score (Q) [Newman and Girvan, 2004]. Modularity was calculated on the graphs constructed for each subject and experimental session using the Louvain algorithm for detection of community structure [Blondel et al., 2008; Rubinov and Sporns, 2011]. As the assumption of normality does not always hold for this graph measure [Godwin et al., 2015], a nonparametric signed rank-sum test was applied on the modularity score to evaluate its change following experimental manipulations (i.e. SD). This process was also repeated following randomization of graph edges (while preserving degree distribution) to validate a state specific change in modularity score.

Group level graphs were constructed by averaging state-specific graphs across subjects in a weighted manner

$$\mathrm{Success(s)} = \begin{cases} 0 \ \ if \ jac\left(G_s^{\mathrm{SR}}, \ G_{-s}^{\mathrm{SD}}\right) < jac\left(G_s^{\mathrm{SR}}, \ G_{-s}^{\mathrm{SR}}\right) \ and \ jac\left(G_s^{\mathrm{SD}}, \ G_{-s}^{\mathrm{SD}}\right) < jac\left(G_s^{\mathrm{SD}}, \ G_{-s}^{\mathrm{SR}}\right) \\ 2 \ \ if \ jac\left(G_s^{\mathrm{SR}}, \ G_{-s}^{\mathrm{SR}}\right) \geq jac\left(G_s^{\mathrm{SR}}, \ G_{-s}^{\mathrm{SD}}\right) \ and \ jac\left(G_s^{\mathrm{SD}}, G_{-s}^{\mathrm{SD}}\right) \geq jac\left(G_s^{\mathrm{SD}}, G_{-s}^{\mathrm{SR}}\right) \\ otherwise \ 1 \end{cases} \quad (2)$$
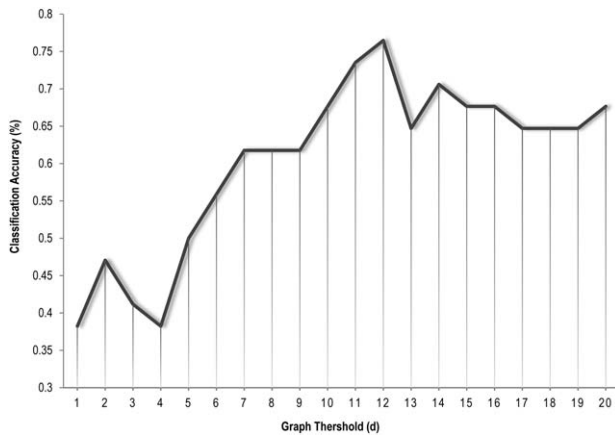
Figure 1.

State prediction accuracy as a function of graph density. Classification accuracy as a function of graph density. Y-axis depicts percent cases of correct SD-SR classification as a function of chosen graph threshold (x-axis). $d = 12$ produced the highest accuracy (0.765) and was therefore used for all subsequent analyses.

[Tagliazucchi et al., 2013]. This averaging resulted in graphs G^{SR} and G^{SD}, in which the weight $w(i,j)$ given to an edge connecting node i with node j, represents the fraction of subject-specific graph in which this connection appeared (e.g. 0.5 if a link is present in 50% of all subjects and 0 if a link is never found). These average graphs, G^{SR} and G^{SD}, were then used to evaluate state-specific modularity structures separately for SR and SD, by applying the weight-conserving Louvain modularity algorithm [Rubinov and Sporns, 2011]. To account for possible instability of the results due to heuristic steps in algorithm implementation (see [Rubinov and Sporns, 2011]), this procedure was repeated 1,000 times for each graph, and the results were merged using the BCT implementation of consensus clustering in complex networks described in [Lancichinetti and Fortunato, 2012]. In addition, for each of the identified group-level modules, a measure of module density was calculated separately for each subject and state, by dividing the number of intramodular connections by the number of all node pairs in the module.

Identified modules were also tested for statistical enrichment of seven predefined functional brain networks (reported in [Yeo et al., 2011]). The principal idea behind enrichment analysis is to examine if a specific class of elements with an established function is much more prevalent within a given group than would be expected by chance. If so this group is suggested to have a non-random association with the established function [Huang et al., 2009]. Such enrichment is assigned with a p-value that is calculated using a hypergeometric test, and can thus be used as a statistically sound way of characterizing groups of neural parcels (see examples in [Lahav et al., 2016; Maron-Katz et al., 2016b]. This analysis was conducted using the RichMind toolbox (http://acgt.cs.tau.ac.il/RichMind [Maron-Katz et al., 2016a]).

To further delineate the changes in functional organization of the brain following SD, we examined the participation coefficient, or the degree to which nodes connect with other nodes outside their assigned module. The participation coefficient provides a measure of a node's importance in intermodular communication. Nodes with high participation indicate regions that contribute to between-module communication [Tagliazucchi et al., 2013]. The participation coefficient of node i is calculated by:

Participation coefficient

$$P_i = 1 - \sum_{j}^{N_M} \left(\frac{k_i^{U_j}}{k_i} \right)^2$$

In this equation, j runs over all modules, k_i is the degree of node i and $k_i^{u_j}$ is the number of links between node i and all nodes of module U_j.

Examining Changes in Graph Modularity in Relation to Behavior/Task Induced Activity

Lastly, in order to examine whether network changes following SD might be associated with behavioral impairments displayed by our subjects, we correlated modular and nodal measurements with cognitive and affective outcomes assessed by PVT task performance and PANAS mood scores, respectively. Given prior evidence for the role of thalamic and motor connectivity in PVT performance following SD [Chee et al., 2008], we examined the correlation between the number of PVT lapses and the density of the relevant somato-motor/salience module across states. To examine changes in mood, we examined both negative and positive PANAS scores as a function of mid-frontal degree, given previous work relating left middle frontal gyrus (MFG) activation to changes in mood [Miller et al., 2013].

Beyond behavioral measures we were also interested to explore whether the observed resting state changes in the limbic module might predict changes in amygdala reactivity during a subsequent emotional distraction task. To that end we conducted a post hoc analysis of the correlation between limbic module density across states with the change in task related amygdala activation. The emotional distraction task, performed following the rest scan in both SD and SR sessions, is an emotional version of the classic N-back task that utilizes neutral and negative images as distractors during the performance of the N-back task. The results of this task were published elsewhere [Simon et al., 2015] and further task details are provided in the Supporting Information.

RESULTS

Selecting an Optimal Graph Density Based on State Prediction Accuracy

An unweighted, undirected graph was generated for each subject and state using a pre-defined link-density (d; the fraction of edges present in the graph). To select the

TABLE I. Top ranking degree-based features used for LOOCV state-prediction

MNI center	AAL label	% Iterations used	SR mean degree (±STD)	SD mean degree (±STD)	hub status (SR→SD)	P value (rank sum)
(45,42,15)	Right middle frontal gyrus	100	14.24 (5.52)	27 (10.02)	0->1	0.0039
(0,–6,6)	Thalamus	100	27.47 (14.85)	13.47 (12.03)	1->0	0.006
(–30,57,3)	Left middle frontal gyrus	100	29.53 (12.41)	15.82 (13.11)	1->0	0.0168
(30,–3,–39)	Right fusiform	94.11	8.18 (8.81)	20.53 (17.51)	No Change	0.0086
(15,21,60)	Right SMA	88.24	36.41 (8.78)	24.41 (11.5)	No Change	0.0129
(21,–9,–18)	Right amygdala	76.47	17.71 (9.45)	29.24 (15.96)	0->1	0.0615

optimal link density, we used leave-one-out cross validation (LOOCV) and classified the SR and SD graphs of the left-out subject under different density values ($d = 0.01–0.2$; 0.01 intervals, see Methods). Figure 1 depicts the accuracy achieved in this procedure. According to this test, $d = 0.12$ produced the highest state classification accuracy (76.5%, $P = 0.0015$, binomial distribution) and was therefore used for all downstream graph analysis.

STATE-PREDICTION OPTIMIZATION USING FEATURE SELECTION

In order to pinpoint the nodes (i.e. ROIs) that contribute most to SD-SR classification accuracy, we repeated the classification procedure using a subset of k nodes, for which nodal degrees exhibited the largest change from SR to SD ($k = 1$ to 182, see Methods). A maximum accuracy of 82.35% ($P = 1.93 \times 10^{-5}$, Binomial distribution) was achieved using only 24 nodes; with specificity and sensitivity of 82.35%. Of these top-ranking nodes, six repeatedly appeared in over 70% of all classification iterations, reflecting the most robust ROIs in sleep state classification. These nodes are listed in Table I and presented in Figure 2.

Our results indicate that ROIs centered in the medial thalamus, the lateral left and right middle frontal gyri, right SMA, right amygdala and right fusiform gyrus significantly modified their nodal degree (i.e. their connectivity) as a function of sleep, thus contributing to improved classification accuracy. Specifically, we revealed a significant decrease in the degree of a node located in the medial thalamus (which was no longer considered a hub following SD), as well as in nodes located in the left lateral MFG and right SMA. A significant increase in nodal degree was found in the right lateral MFG (considered a hub only following SD) as well as in the right fusiform. Notably a
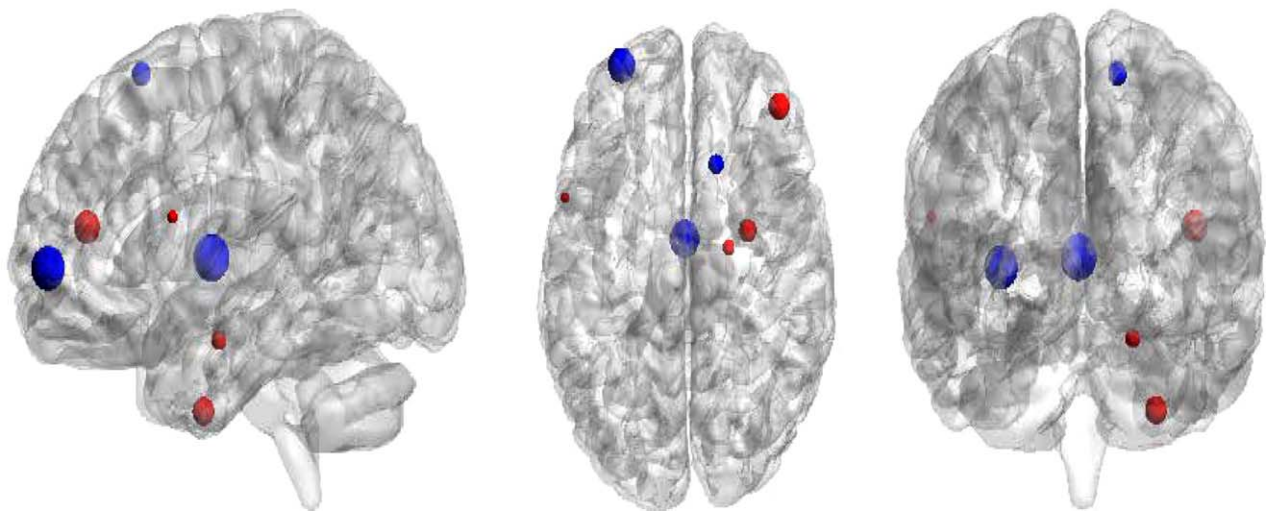

Figure 2.
Top ranking nodes. The most contributing nodes to SD-SR classification accuracy. Regions are depicted on a schematic three-dimensional brain; with circle size representing the magnitude of change across states (see Table I). Blue (red) circles represent regions that are significantly less (more) connected following SD, respectively. [Color figure can be viewed at wileyonlinelibrary.com]
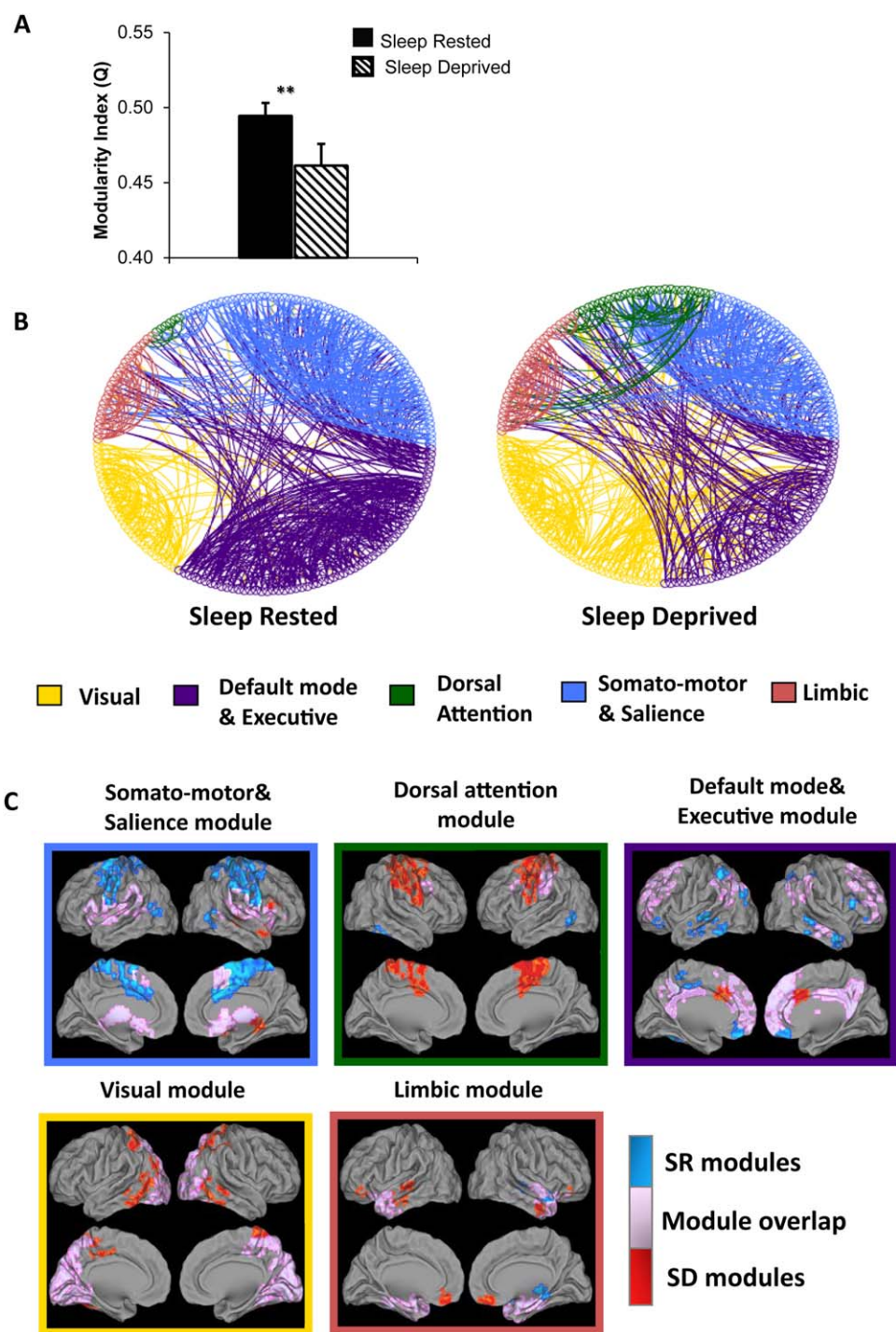
Figure 3.

Changes in modularity structure following SD. Changes in modular structure following SD. (**A**) Modularity scores (*Q*) decreased significantly across all participants following SD. (**B**) This is also visualized in a circular graph of connectivity across all nodes (for visual purposes only top 50% links are displayed). (**C**) The five functional modules revealed in each state. Regions colored in blue (red) were assigned to the specific module only during SR (SD) sessions, respectively. Overlapping regions (identical across states) are depicted in purple. [Color figure can be viewed at wileyonlinelibrary.com]

TABLE II. Functional modules

SR module assignment	SR module coverage (network parcels out of all module parcels)	SD module assignment	SD module coverage (network parcels out of all module parcels)	SD-SR module overlap (Jaccard score)
Visual network	23/30 ($q = 8.55$E-14)	Visual network	26/45; ($q = 2.48$E-12)	0.67
Frontoparietal control network & default mode network	21/55 ($q = 4.67$E-8). 25/55 ($q = 2.3$E-8)	Frontoparietal control network & default mode network	19/42 ($q = 3.41$E-8); 16/42 ($q = 0.0014$)	0.64
Somato-motor network & ventral attention network	21/62($q = 22.24$E-11) 16/62 ($q = 1.18$E-4)	Ventral attention network	13/41 ($q = 1.76$E-4)	0.58
Dorsal attention network	6/14 ($q = 8.19$E-5)	Dorsal attention network & somato-motor network	5/25 ($q = 0.025$); 11/25 ($q = 1.73$E-5)	0.18
Limbic network	8/21 ($q = 1.03$E-6)	Limbic network & default mode network	9/29 ($q = 9$E-7); 12/29 ($q = 0.0043$)	0.72

node located in the right amygdala demonstrated a marginally significant increase in nodal degree ($P = 0.06$), considered a hub only following SD.

We further examined the contribution of specific functional connectivity pairs (i.e. edges instead of nodes) to sleep-state classification using top ranking edges ($k = 1$–500). This analysis achieved lower accuracy levels with higher number of features ($k = 152$, accuracy $= 73.53\%$) and is further detailed in the Supporting Information.

SD Induced Changes in Network Modularity

Examining modularity scores between states, we observed a significant decrease across subjects (Q, mean (ΔQ) $= -0.033$, $P < 0.01$ Wilcoxon-signed rank sum test; see Fig. 3a). Notably, a significant decrease in modularity following SD was observed across all graph densities ($0.1 < d < 0.19$; 0.01 intervals). Furthermore, when randomizing the graphs (while preserving degree distribution) no significant differences in modularity were found between sleep states ($q > 0.7$, see Methods for further details).

To explore consistent changes in modularity membership across all subjects, we created a "group level" graph by averaging state-specific graphs across subjects using the weighted version of the Louvian algorithm (see Methods). As with individual graphs, these group-level graphs also revealed a decrease in modularity score following SD (mean over 1,000 repetitions (ΔQ) $= -0.03$; a decrease of 9% from original Q; repetitions were used for stabilization purposes, see Methods). These changes are presented in Figure 3 and Table II (for a full list of regions within each module, also see Supporting Information Table S1). This analysis revealed five modules in each experimental session without a change in the total number of modules as a function of sleep, also reported in [Tagliazucchi et al., 2013].

In order to accurately characterize the functional "identity" of each module in a statistically sound manner, we applied an enrichment analysis on each module using

seven predefined functional brain networks as reported in [Yeo et al., 2011]. Table II depicts the functional networks that had a significant overlap with our reported modules. These networks include: the visual network (the visual module), the default mode and frontoparietal executive networks (the FP-DMN module), the sensory-motor/ saliency networks (the SMN/saliency module), the dorsal attention network (the DAttention module) and the limbic network (the limbic module).

SD Induced Changes in Module Membership

To identify which modules were most affected by SD, we examined the changes in module membership across SR and SD states. Similar to the state-classification analysis, changes in module membership were mostly centered around several main hubs affected by SD. The thalamus, a major hub of the somatomotor/salience module, lost most of its cortical connections following SD, associated with a substantial reduction in the density of the SMN-salience module. In accordance with altered amygdala connectivity as reported above, we further revealed an increase in limbic module density following SD, which now included regions such as the ventromedial PFC typically associated with the default mode network (this region is in fact part of the DMN module in the SR session). As a result DMN module density was further reduced following SD.

SD Induced Changes in Intermodular Connectivity

In order to examine which nodes were most influential in modifying the network's modularity structure, we calculated each node's participation coefficient (see Methods). High participation coefficient indicates that a node has many connections outside of its assigned module therefore participating in intermodular connectivity. In accordance with a breakdown of modular organization following SD, the average participation coefficient was significantly higher without
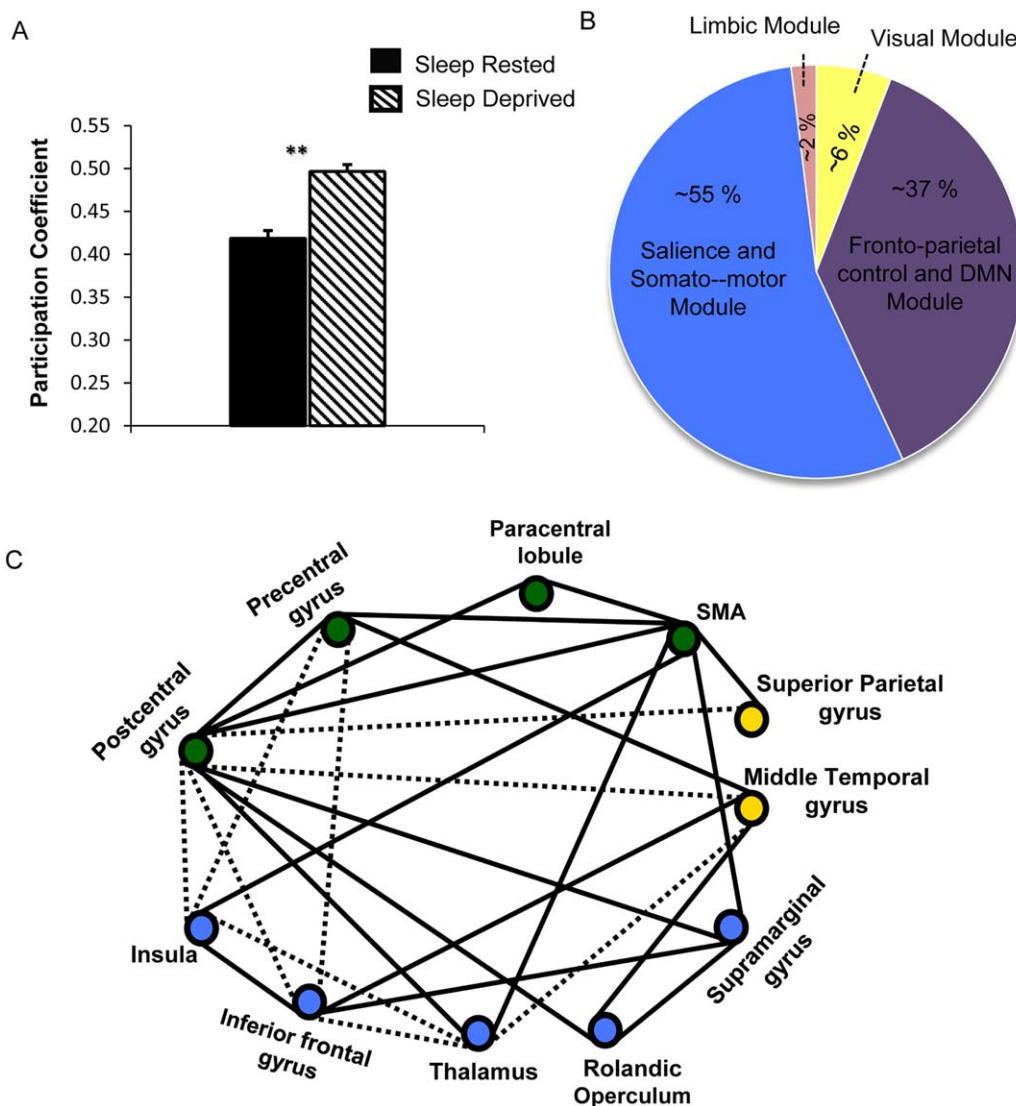
A

B

C

Figure 4.

Participation coefficient scores. Changes in participation coefficients across sleep states. (**A**) A significant increase in mean participation coefficient scores across all nodes following SD. (**B**) The distribution of nodes that significantly modified their participation score following SD (SR module assignment is displayed). The majority of nodes undergoing a significant change in intermodular connectivity belong to the FP-DMN module as well as to the SMN-salience module. (**C**) Changes in SMN-salience

module structure following SD. Solid lines represent stable intramodular links across states, while dashed lines represent links lost following SD. For display purposes, only one node for each pair of bilateral regions is shown, as well as edges that appear in at least 80% of the subjects. Node colors represent module assignment following SD (blue: salience module; yellow: visual module; green: SMN-dorsal attention module). **$P < 0.001$. [Color figure can be viewed at wileyonlinelibrary.com]

sleep (P, mean $(\Delta P) = 0.065$, $P < 0.001$, Wilcoxon-signed rank sum test; see Fig. 4a). We further examined which nodes differed in their participation score following SD. This analysis revealed 45 nodes that demonstrated a significant increase in participation score (mean $(\Delta P) = 0.18$; $q < 0.05$, FDR corrected). The distribution of these nodes according to their functional module is depicted in Figure 4b.

Similar to the modularity analysis, our results reveal that, the FP-DMN module as well as the SMN-Saliency module underwent the largest alterations in participation scores, demonstrating a prominent rearrangement of their modular structure without sleep.

Notably, modularity scores could be affected by both changes in intermodular connectivity (assessed by the

participation coefficient) or by a decrease in intramodular connectivity (assessed by intramodular degree), which would indicate a breakdown of the modules themselves. Interestingly, our analysis did not find a significant difference in intramodular connectivity (examining normalized node score; $q > 0.6$, or actual node degree; $q > 0.2$), suggesting that the changes in the modularity structure of the network are mostly due to a loss of functional segregation. Interestingly, the average clustering coefficient and path length of the network, which also measure functional segregation and integration respectively, did not differ as a function of sleep (Wilcoxon's signed-rank test, both $P > 0.76$). However, unlike modularity and participation coefficient, neither path length nor clustering coefficient take into account module membership and are thus mostly sensitive to changes in individual node connectivity. The fact that only measures that are particularly sensitive to module membership, were altered by SD, strongly suggests that sleep loss is associated with a breakdown of the brain's global functional organization leading to a loss of functional segregation.

Impact of Sleep Deprivation on Task Performance and Mood

SD was associated with an increase in attentional lapses, as indicated by the Psychomotor Vigilance Task (PVT) measured at 7 a.m. of each session ($M = 2.94 \pm 2.49$ to $M = 10.06 \pm 6.86$; $P < 0.0005$) as well as across the SD night (measured at 23 p.m. and 7 a.m. of the SD session, $M = 2.88 \pm 2.37$ to $M = 10.06 \pm 6.86$; $P < 0.0005$). Participants' mood was also impaired by SD, as assessed by the PANAS mood scores. PANAS scores revealed a significant decline in the positive scale following SD compared to the SR session ($M = 2.86 \pm 0.65$ to $M = 2.01 \pm 0.85$; $P < 0.0005$) as well as a slight increase in the negative scale ($M = 1.3 \pm 0.28$ to $M = 1.59 \pm 0.56$; $P < 0.05$).

Network Changes in Relation to Behavior and Task Induced Activity

Lastly, in order to examine the link between the observed network changes following SD and cognitive and affective outcomes, we correlated modular and nodal measurements with PVT and PANAS scores, respectively. First, given the psychomotor nature of the PVT task (Drummond et al., 2005] we examined whether the observed decline in the SMN-salience module density might be associated with the reported decrease in task performance following SD. Indeed, the decline in PVT performance (indicated by increased number of attentional lapses) was significantly correlated with the decrease in SMN-salience module density ($\rho = -0.55$, $P < 0.02$; see Fig. 5a). This finding suggests that a breakdown of the SMN-salience module (specifically a disconnection of

motor regions, see Table II and Fig. 4) was associated with impaired sustained attention during the task.

Second, we found robust changes in bilateral mid-frontal degree following SD (see Table I), which suggests a shift from left to right dominance in lateral mid frontal connectivity patterns. In light of previous work relating the left middle frontal gyrus (MFG) to positive mood [Miller et al., 2013], we examined whether the decline in left MFG degree is associated with participants' altered mood scores following SD. As mentioned above, both the negative and positive scales of the PANAS questionnaire were affected by sleep deprivation, and therefore both were examined as a function of change in left MFG degree across states (SD–SR). Only the increase in negative mood was found to be significantly anticorrelated with the change in left MFG degree ($\rho = -0.50$, $P < 0.05$; see Fig. 5b; for positive mood $\rho = 0.05$, $P > 0.8$), suggesting that a decrease in left MFG connectivity is associated with worse mood following SD. Notably, the change in negative mood was further found to be positively correlated with the change in right MFG degree ($\rho = 0.47$, $P = 0.05$) suggesting the opposite direction (i.e. that a more connected right MFG is associated with worse negative mood following SD). Altogether, these findings support the interaction between bilateral mid-frontal connectivity and mood (see review by [Miller et al., 2013]), and suggest that beyond changes to the limbic module, connectivity pattern of the left and right MFG might also be involved in the affective impact of sleep loss.

Lastly, we wished to evaluate whether the observed changes in limbic module density could predict activity levels during subsequent task performance in a specific region of interest. Given our previous work on task-related hyperactivation of the amygdala following SD [Simon et al., 2015], we examined whether changes in limbic module density might be associated with amygdala activity during a subsequent emotional distraction task (for further details on the task see Methods and Supporting Information). As expected, the increase in limbic module density following SD was significantly correlated with the increase in the reported left amygdala response to task stimuli ($\rho = 0.62$; $P < 0.02$; see Fig. 5b). This finding suggests that hyperactivity of affective brain regions following SD is reflected in altered connectivity patterns of the limbic network even prior to task performance.

DISCUSSION

Using graph-based analysis, we were able to capture a large-scale change in the brain's modular organization induced by lack of sleep. Our data-driven whole-brain approach revealed that sleep loss is associated with significant changes in the modularity structure of key emotional, salience and default mode regions, the latter two principally leading the decrease in the brain's modular organization. These changes were further associated with impaired
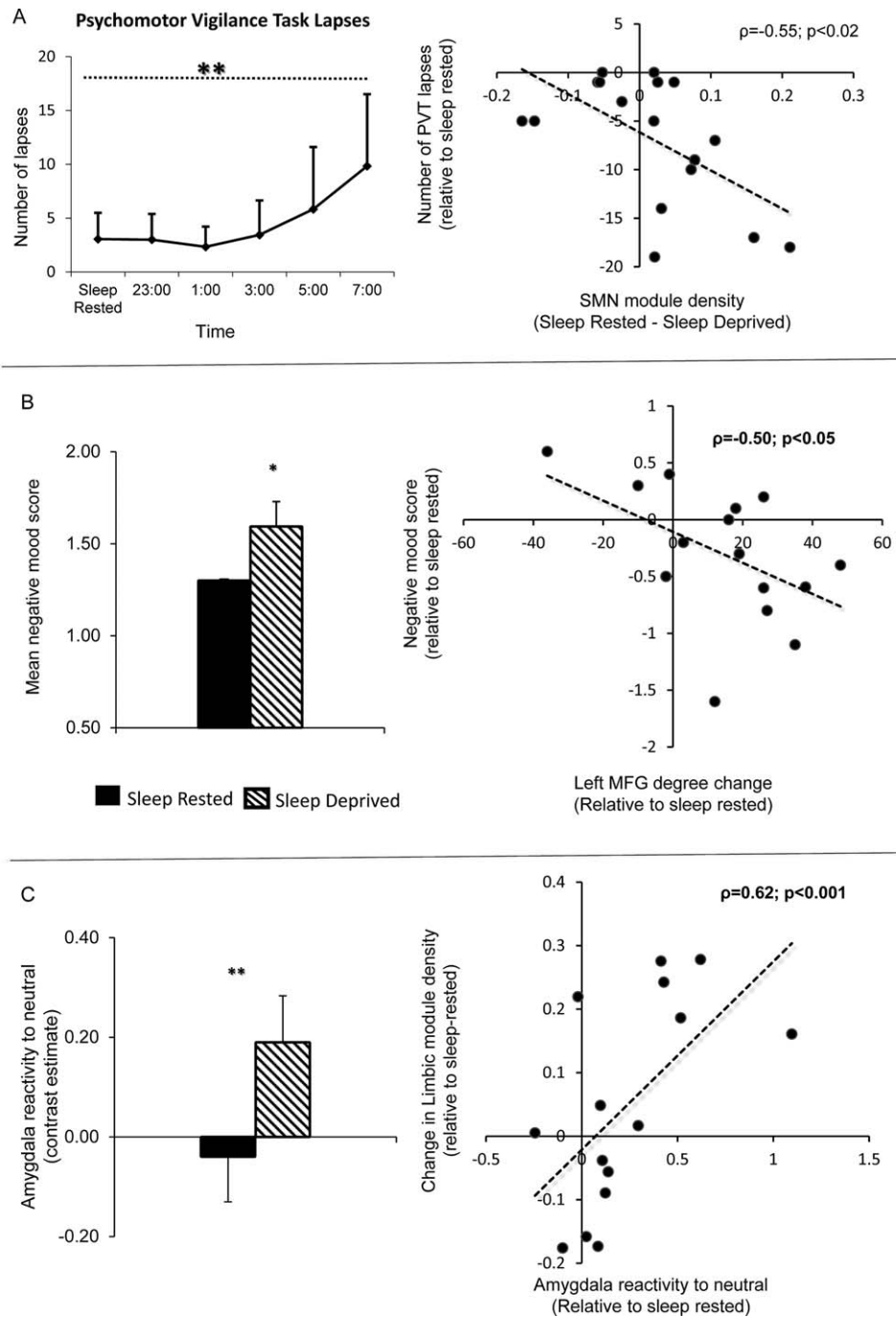
Figure 5.

Modular change and relation to behavior. Changes in modular structure following SD and relation to behavior and task reactivity. (**A**) The mean number of PVT lapses across the SD night (left) and its correlation with SMN-salience module density (right). The negative correlation suggests that a sparser SMN module was associated with worse task performance. (**B**) A significant increase in negative mood following SD (left) and a negative correlation between worse negative mood and a decrease in left MFG degree (right). (**C**) Left amygdala reactivity to neutral stimuli during the emotional N-Back task in SR and SD (left) and correlation of amygdala reactivity with increase in limbic module density (right). The positive correlation suggests that sleep-related changes in limbic module connectivity during rest could predict amygdala reactivity during subsequent task performance. *$P < 0.05$, **$P < 0.0001$.

behavioral and neural outcomes known to occur without sleep. Specifically, we identified a significant association between limbic module density during rest and hyper activation of the amygdala during a subsequent emotional task as well as an association between mid-frontal degree patterns and worse negative mood.

To begin with, we demonstrated that both modularity and participation coefficient measures, which quantify the integration/segregation balance in large-scale networks [Godwin et al., 2015], are altered by sleep deprivation. These alterations indicate a breakdown of the brain's modular organization, suggesting that the human brain moves towards a more random like organization without sleep, ultimately reducing functional segregation [Kitzbichler et al., 2011]. In accordance, decreased modularity scores have been reported in states of normal aging [Meunier et al., 2009], schizophrenia [Alexander-Bloch et al., 2010], and Alzheimer's disease [de Haan et al., 2012]. In contrast, increased modularity was recently reported in the unconscious states of deep sleep (stages N2 and N3) suggesting that sleep might increase functional segregation [Boly et al., 2012; Tagliazucchi et al., 2013] possibly resetting the brain's integration/segregation balance back to an optimal state.

Notably, whether increased modularity is always a marker for improved function has recently been challenged by a neuroimaging study exploring brain modularity during masked visual perception [Godwin et al., 2015]. The authors demonstrated that aware versus unaware detection of visual stimuli was associated with reduced modularity across the entire brain, suggesting that reduced modularity might enable conscious awareness through a temporary increase in functional integration (as opposed to functional segregation which is supported by increased modularity). Future studies utilizing graph theory analysis across different functional states (including different states of consciousness) could prove valuable to further address this interesting topic.

In addition to whole brain modifications in modularity we revealed that SD elicited a prominent change in the connectivity patterns of key nodes within the salience and limbic networks. The thalamus, known for its central role in arousal regulation [Schiff, 2008] and in attention and arousal interactions [Portas et al., 1998], was found to be significantly less connected following sleep loss, ultimately losing its hub status in the sleep deprived graph (see Table I). In accordance with a recent study that examined resting thalamic connectivity following sleep deprivation we further observed a reduction of thalamic connectivity with bilateral midtemporal regions [Shao et al., 2013] (also see Fig. 4), and were further able to associate the decrease in thalamic module density (i.e. the SMN-salience module) with attentional lapses as assessed by the PVT (see Fig. 5). Similarly, sleep deprivation was previously associated with reduced thalamic activity during lapses in PVT [Chee et al., 2008] as well as reduced resting metabolic activity in the thalamus during PET recordings [Thomas et al., 2000; Wu et al., 1991].

Interestingly, reductions in thalamo-cortical connectivity have also been demonstrated during NREM sleep [Tagliazucchi et al., 2013], propofol-induced unconsciousness [Guldenmund et al., 2013], light anesthesia [Akeju et al., 2016], and in presleep deep relaxation [Kinreich et al., 2014]. These findings imply that the sleep-deprived brain might be susceptible to short sleep onsets (i.e. sleep intrusion [Cirelli and Tononi, 2008]), while still behaviorally awake, in line with recent suggestions [Vyazovskiy et al., 2011]. This hypothesis is further supported by a recent study demonstrating a significant reduction in thalamic degree only during the first NREM stage of sleep onset (N1), arguably the closest state to sleep deprivation [Spoormaker et al., 2010; Tagliazucchi et al., 2013; Yeo et al., 2015].

Our findings also reflect robust changes in the FP-DMN module following SD, expressed in increased participation coefficient scores (see Fig. 4), reduced module density and changes in module membership, specifically within the DMN. Indeed, the DMN has consistently been shown as sensitive to sleep manipulations. For instance, Gujar et al. demonstrated that one night of sleep loss triggers a marked reduction in DMN deactivation during task performance further associated with unsuccessful task trials [Gujar et al., 2010]. SD has further induced a reduction in DMN connectivity [Kaufmann et al., 2016; Yeo et al., 2015] ultimately leading to a split within the DMN module, mostly led by a breakdown of anterior-posterior DMN connectivity [Wang et al., 2015]. Interestingly, sleep studies have also reported a reduction in posterior-anterior connectivity of the DMN, during the deeper stages of NREM sleep (i.e. N3 and N4, [Horovitz et al., 2009; Sämann et al., 2011; Tagliazucchi et al., 2013]), again suggesting that the sleep deprived brain is highly susceptible to sleep-like changes in brain function while still behaviorally awake. One of the main features of DMN connectivity, i.e. its functional de-coupling (or anti correlated activity) from the brain's attentional networks, has also been reported to weaken following SD. This functional decoupling, thought to reflect an adaptive mechanism of attention regulation [Fox et al., 2009], has been reduced following both complete and partial sleep deprivation [Bosch et al., 2013; De Havas et al., 2012; Sämann et al., 2010], leading to a significant reduction in the brain's functional segregation [De Havas et al., 2012]. In accordance, Yeo et al. were able to associate resilience to sleep deprivation (assessed via improved task performance following SD) with the level of preserved DMN anti correlations, demonstrating the importance of intact functional segregation to counteract the detrimental effects of sleep loss [Yeo et al., 2015].

In accordance with the impact of SD on emotional states, we further revealed a decrease in left MFG degree that was significantly correlated with the change in subjects' negative mood (see Fig. 5b). The lateralized effect of left and right mid-frontal regions on affect has long been described in both healthy controls [Miller et al., 2013] as

well as in patients suffering from mood disorders [Herrington et al., 2010]. Though still debated [Wager et al., 2003], positive affect has generally been associated with greater left over right activity while a decrease in left MFG activity has been associated with negative affect, a distinction further supported by lesion studies [Hama et al., 2007]. In accordance, we revealed a significant shift in lateralized mid frontal dominance as a function of sleep; while left MFG was considered a hub in the SR network, its connectivity decreased following SD, leading to a loss of its hub status. The exact opposite occurred in the right MFG, which was only considered a hub following SD (see Fig. 2). These findings suggest that the negative impact of sleep loss on emotional well-being could stem from dynamic changes in mid-frontal connectivity in addition to changes within the limbic network.

Lastly, affective changes as a result of SD were also indicated by the increase in limbic module density and in particular right amygdala connectivity (regarded as a hub only following SD; see also [Shao et al., 2014]). Interestingly, we were able to associate the increase in limbic module density to task-related changes in amygdala activity during subsequent performance of an emotional distraction task (see Fig. 5c). This finding supports a functional link between spontaneous neural activity in the limbic circuit and prospective emotional control during task performance, which enables to predict the impact of SD on emotional processing even during rest [Raichle, 2011]. Altogether, these findings support a profound change in emotional processing elicited by sleep loss as indicated by both task related activity as well as resting state measures of graph connectivity. This association is particularly relevant to the intimate link between disturbed sleep and various depressive, manic, anxious and/or psychotic disorders (see review by [Goldstein and Walker, 2014] and supports the invaluable importance of sleep to a healthy emotional state.

To conclude, using a data driven approach we were able to detect robust changes in the functional segregation of the human brain, leading to a more random-like structure without sleep. These changes were centered on key regions of the limbic, salience and default mode networks, further associated with impairments in cognitive task performance, task-related amygdala reactivity as well as in participants' emotional state following SD. These findings confirm the global impact of sleep loss on the brain's functional architecture detected even prior to task performance and indirectly point to the importance of sleep in preserving the functional segregation of the human brain.

REFERENCES

Akeju O, Song AH, Hamilos AE, Pavone KJ, Flores FJ, Brown EN, Purdon PL (2016): Electroencephalogram signatures of ketamine anesthesia-induced unconsciousness. Clin Neurophysiol 127:2414–2422.

Alexander-Bloch AF, Gogtay N, Meunier D, Birn R, Clasen L, Lalonde F, Lenroot R, Giedd J, Bullmore ET (2010): Disrupted modularity and local connectivity of brain functional networks in childhood-onset schizophrenia. Front Syst Neurosci 4:147.

Barnes A, Bullmore ET, Suckling J (2009): Endogenous human brain dynamics recover slowly following cognitive effort. PLoS One 4:e6626.

Blondel VD, Guillaume J-L, Lambiotte R, Lefebvre E (2008): Fast unfolding of communities in large networks. J Stat Mech 2008: P10008.

Boly M, Perlbarg V, Marrelec G, Schabus M, Laureys S, Doyon J, Pélégrini-Issac M, Maquet P, Benali H (2012): Hierarchical clustering of brain activity during human nonrapid eye movement sleep. Proc Natl Acad Sci USA 109:5856–5861.

Bosch OG, Rihm JS, Scheidegger M, Landolt H-P, Stämpfli P, Brakowski J, Esposito F, Rasch B, Seifritz E (2013): Sleep deprivation increases dorsal nexus connectivity to the dorsolateral prefrontal cortex in humans. Proc Natl Acad Sci USA 110: 19597–19602.

Bullmore E, Sporns O (2009): Complex brain networks: graph theoretical analysis of structural and functional systems. Nat Rev Neurosci 10:186–198.

Chee MW, Tan JC, Zheng H, Parimal S, Weissman DH, Zagorodnov V, Dinges DF (2008): Lapsing during sleep deprivation is associated with distributed changes in brain activation. J Neurosci 28:5519–5528.

Cirelli C, Tononi G (2008): Is sleep essential? PLoS Biol 6:e216.

Craddock RC, James GA, Holtzheimer PE, Hu XP, Mayberg HS (2012): A whole brain fMRI atlas generated via spatially constrained spectral clustering. Hum Brain Mapp 33:1914–1928.

de Haan W, van der Flier WM, Koene T, Smits LL, Scheltens P, Stam CJ (2012): Disrupted modular brain dynamics reflect cognitive dysfunction in Alzheimer's disease. Neuroimage 59: 3085–3093.

De Havas JA, Parimal S, Soon CS, Chee MW (2012): Sleep deprivation reduces default mode network connectivity and anticorrelation during rest and task performance. Neuroimage 59: 1745–1751.

Dinges DF, Pack F, Williams K, Gillen KA, Powell JW, Ott GE, Aptowicz C, Pack AI (1997): Cumulative sleepiness, mood disturbance and psychomotor vigilance performance decrements during aweek of sleep restricted to 4-5 hours per night. J Sleep Res Sleep Med 20:267–277.

Drummond SP, Bischoff-Grethe A, Dinges DF, Ayalon L, Mednick SC, Meloy M (2005): The neural basis of the psychomotor vigilance task. Sleep 28:1059.

Fox MD, Zhang D, Snyder AZ, Raichle ME (2009): The global signal and observed anticorrelated resting state brain networks. J Neurophysiol 101:3270–3283.

Gao L, Bai L, Zhang Y, Dai X-J, Netra R, Min Y, Zhou F, Niu C, Dun W, Gong H (2015): Frequency-dependent changes of local resting oscillations in sleep-deprived brain. PLoS One 10: e0120323.

Godwin D, Barry RL, Marois R (2015): Breakdown of the brain's functional network modularity with awareness. Proc Natl Acad Sci USA 112:3799–3804.

Goldstein AN, Walker MP (2014): The role of sleep in emotional brain function. Annu Rev Clin Psychol 10:679.

Greicius MD, Menon V (2004): Default-mode activity during a passive sensory task: uncoupled from deactivation but impacting activation. J Cogn Neurosci 16:1484–1492.

Gujar N, Yoo S-S, Hu P, Walker MP (2010): The unrested resting brain: sleep deprivation alters activity within the default-mode network. J Cogn Neurosci 22:1637–1648.

Guldenmund P, Demertzi A, Boveroux P, Boly M, Vanhaudenhuyse A, Bruno M-A, Gosseries O, Noirhomme Q, Brichant J-F, Bonhomme V (2013): Thalamus, brainstem and salience network connectivity changes during propofol-induced sedation and unconsciousness. Brain Connect 3: 273–285.

Hama S, Yamashita H, Shigenobu M, Watanabe A, Kurisu K, Yamawaki S, Kitaoka T (2007): Post-stroke affective or apathetic depression and lesion location: Left frontal lobe and bilateral basal ganglia. Eur Arch Psychiatry Clin Neurosci 257:149–152.

Herrington JD, Heller W, Mohanty A, Engels AS, Banich MT, Webb AG, Miller GA (2010): Localization of asymmetric brain function in emotion and depression. Psychophysiology 47: 442–454.

Horovitz SG, Braun AR, Carr WS, Picchioni D, Balkin TJ, Fukunaga M, Duyn JH (2009): Decoupling of the brain's default mode network during deep sleep. Proc Natl Acad Sci USA 106:11376–11381.

Huang DW, Sherman BT, Lempicki RA (2009): Bioinformatics enrichment tools: Paths toward the comprehensive functional analysis of large gene lists. Nucleic Acids Res 37:1–13.

Joyce KE, Hayasaka S, Laurienti PJ (2013): The human functional brain network demonstrates structural and dynamical resilience to targeted attack. PLoS Comput Biol 9:e1002885.

Kaufmann T, Elvsåshagen T, Alnæs D, Zak N, Pedersen PØ, Norbom LB, Quraishi SH, Tagliazucchi E, Laufs H, Bjørnerud A (2016): The brain functional connectome is robustly altered by lack of sleep. NeuroImage 127:324–332.

Kinreich S, Podlipsky I, Jamshy S, Intrator N, Hendler T (2014): Neural dynamics necessary and sufficient for transition into pre-sleep induced by EEG neurofeedback. Neuroimage 97: 19–28.

Kitzbichler MG, Henson RN, Smith ML, Nathan PJ, Bullmore ET (2011): Cognitive effort drives workspace configuration of human brain functional networks. J Neurosci 31:8259–8270.

Lahav N, Ksherim B, Ben-Simon E, Maron-Katz A, Cohen R, Havlin S (2016): K-shell decomposition reveals hierarchical cortical organization of the human brain. N J Phys 18:083013.

Lancichinetti A, Fortunato S (2012): Consensus clustering in complex networks. Sci Rep 2:

Laurienti PJ (2004): Deactivations, global signal, and the default mode of brain function. J Cogn Neurosci 16:1481–1483.

Lee Rodgers J, Nicewander WA (1988): Thirteen ways to look at the correlation coefficient. Am Stat 42:59–66.

Lei Y, Shao Y, Wang L, Ye E, Jin X, Zou F, Zhai T, Li W, Yang Z (2015): Altered superficial amygdala–cortical functional link in resting state after 36 hours of total sleep deprivation. J Neurosci Res 93:1795–1803.

Liang X, Zou Q, He Y, Yang Y (2013): Coupling of functional connectivity and regional cerebral blood flow reveals a physiological basis for network hubs of the human brain. Proc Natl Acad Sci USA 110:1929–1934.

Maldjian JA, Laurienti PJ, Kraft RA, Burdette JH (2003): An automated method for neuroanatomic and cytoarchitectonic atlas-based interrogation of fMRI data sets. NeuroImage 19: 1233–1239.

Maron-Katz A, Amar D, Simon EB, Hendler T, Shamir R (2016a): RichMind: A Tool for Improved Inference from Large-Scale Neuroimaging Results. PLoS One 11:e0159643.

Maron-Katz A, Vaisvaser S, Lin T, Hendler T, Shamir R (2016b): A large-scale perspective on stress-induced alterations in resting-state networks. Sci Rep 6:21503.

Meunier D, Achard S, Morcom A, Bullmore E (2009): Age-related changes in modular organization of human brain functional networks. Neuroimage 44:715–723.

Miller G, Crocker L, Spielberg J, Infantolino Z, Heller W (2013): Issues in Localization of brain function: The case of lateralized frontal cortex in cognition, emotion, and psychopathology. Front Integr Neurosci 7:2. Available at: http://journal.frontiersin.org/article/10.3389/fnint.2013.00002.

Mueller ST, Piper BJ (2014): The psychology experiment building language (PEBL) and PEBL test battery. J Neurosci Methods 222:250–259.

Murphy K, Birn RM, Handwerker DA, Jones TB, Bandettini PA (2009): The impact of global signal regression on resting state correlations: are anti-correlated networks introduced? Neuroimage 44:893–905.

Newman ME, Girvan M (2004): Finding and evaluating community structure in networks. Phys Rev E 69:026113.

Pilcher JJ, Huffcutt AJ. (1996): Effects of sleep deprivation on performance: A meta-analysis. J Sleep Res Sleep Med 19:318–326.

Portas CM, Rees G, Howseman A, Josephs O, Turner R, Frith CD (1998): A specific role for the thalamus in mediating the interaction of attention and arousal in humans. J Neurosci 18:8979–8989.

Power JD, Barnes KA, Snyder AZ, Schlaggar BL, Petersen SE (2012): Spurious but systematic correlations in functional connectivity MRI networks arise from subject motion. Neuroimage 59:2142–2154.

Power JD, Mitra A, Laumann TO, Snyder AZ, Schlaggar BL, Petersen SE (2014): Methods to detect, characterize, and remove motion artifact in resting state fMRI. Neuroimage 84: 320–341.

Raichle ME (2011): The restless brain. Brain Connect 1:3–12.

Rubinov M, Sporns O (2010): Complex network measures of brain connectivity: Uses and interpretations. NeuroImage 52: 1059–1069.

Rubinov M, Sporns O (2011): Weight-conserving characterization of complex functional brain networks. NeuroImage 56:2068–2079.

Sämann PG, Tully C, Spoormaker VI, Wetter TC, Holsboer F, Wehrle R, Czisch M (2010): Increased sleep pressure reduces resting state functional connectivity. Magn Reson Mater Phys Biol Med 23:375–389.

Sämann PG, Wehrle R, Hoehn D, Spoormaker VI, Peters H, Tully C, Holsboer F, Czisch M (2011): Development of the brain's default mode network from wakefulness to slow wave sleep. Cereb Cortex 21:2082–2093.

Schiff ND (2008): Central thalamic contributions to arousal regulation and neurological disorders of consciousness. Ann NY Acad Sci 1129:105–118.

Shao Y, Lei Y, Wang L, Zhai T, Jin X, Ni W, Yang Y, Tan S, Wen B, Ye E (2014): Altered resting-state amygdala functional connectivity after 36 hours of total sleep deprivation. PLoS One 9:e112222.

Shao Y, Wang L, Ye E, Jin X, Ni W, Yang Y, Wen B, Hu D, Yang Z (2013): Decreased thalamocortical functional connectivity after 36 hours of total sleep deprivation: Evidence from resting state fMRI. PLoS One 8:e78830.

Simon EB, Oren N, Sharon H, Kirschner A, Goldway N, Okon-Singer H, Tauman R, Deweese MM, Keil A, Hendler T (2015): Losing neutrality: The neural basis of impaired emotional control without sleep. J Neurosci 35:13194–13205.

Song X-W, Dong Z-Y, Long X-Y, Li S-F, Zuo X-N, Zhu C-Z, He Y, Yan C-G, Zang Y-F (2011): REST: A toolkit for resting-state functional magnetic resonance imaging data processing. PLoS One 6:e25031.

Spoormaker VI, Schröter MS, Gleiser PM, Andrade KC, Dresler M, Wehrle R, Sämann PG, Czisch M (2010): Development of a large-scale functional brain network during human non-rapid eye movement sleep. J Neurosci 30:11379–11387.

Stamatakis EA, Adapa RM, Absalom AR, Menon DK (2010): Changes in resting neural connectivity during propofol sedation. PLoS One 5:e14224.

Tagliazucchi E, Von Wegner F, Morzelewski A, Brodbeck V, Borisov S, Jahnke K, Laufs H (2013): Large-scale brain functional modularity is reflected in slow electroencephalographic rhythms across the human non-rapid eye movement sleep cycle. Neuroimage 70:327–339.

Thomas M, Sing H, Belenky G, Holcomb H, Mayberg H, Dannals R, Wagner J, Thorne D, Popp K, Rowland L (2000): Neural basis of alertness and cognitive performance impairments during sleepiness. I. Effects of 24 h of sleep deprivation on waking human regional brain activity. J Sleep Res 9:335–352.

van den Heuvel MP, Stam CJ, Boersma M, Pol HH (2008): Small-world and scale-free organization of voxel-based resting-state functional connectivity in the human brain. Neuroimage 43:528–539.

Vyazovskiy VV, Olcese U, Hanlon EC, Nir Y, Cirelli C, Tononi G (2011): Local sleep in awake rats. Nature 472:443–447.

Wager TD, Phan KL, Liberzon I, Taylor SF (2003): Valence, gender, and lateralization of functional brain anatomy in emotion: A meta-analysis of findings from neuroimaging. Neuroimage 19:513–531.

Wang Y, Liu H, Hitchman G, Lei X (2015): Module number of default mode network: Inter-subject variability and effects of sleep deprivation. Brain Res 1596:69–78.

Watson D, Clark LA, Tellegen A (1988): Development and validation of brief measures of positive and negative affect: the PANAS scales. J Person Soc Psychol 54:1063–1070.

Wong CW, Olafsson V, Tal O, Liu TT (2013): The amplitude of the resting-state fMRI global signal is related to EEG vigilance measures. Neuroimage 83:983–990.

Wu JC, Gillin JC, Buchsbaum MS, Hershey T, et al. (1991): The effect of sleep deprivation on cerebral glucose metabolic rate in normal humans assessed with positron emission tomography. J Sleep Res Sleep Med 14:155–162.

Yeo BT, Krienen FM, Sepulcre J, Sabuncu MR, Lashkari D, Hollinshead M, Roffman JL, Smoller JW, Zöllei L, Polimeni JR (2011): The organization of the human cerebral cortex estimated by intrinsic functional connectivity. J Neurophysiol 106:1125–1165.

Yeo BT, Tandi J, Chee MW (2015): Functional connectivity during rested wakefulness predicts vulnerability to sleep deprivation. NeuroImage 111:147–158.

Yoo S-S, Gujar N, Hu P, Jolesz FA, Walker MP (2007): The human emotional brain without sleep—A prefrontal amygdala disconnect. Curr Biol 17:R877–R878.

Zohar D, Tzischinsky O, Epstein R, Lavie P (2005): The effects of sleep loss on medical residents' emotional reactions to work events: a cognitive-energy model. Sleep 28:47–54.